VOLUME 16
NUMBER 2
JUNE 2003

Physics Essays

An International Journal Dedicated to
Fundamental Questions in Physics

A Physical Model of the Electron According to the Basic Structures of Matter Hypothesis

Stoyan Sarg

Abstract

A physical model of the electron is suggested according to the basic structures of matter (BSM) hypothesis. BSM is based on an alternative concept about the physical vacuum, assuming that space contains an underlying grid structure of nodes formed of superdense subelementary particles, which are also involved in the structure of the elementary particles. The proposed grid structure is formed of vibrating nodes that possess quantum features and energy well. It is admitted that this hypothetical structure could account for the missing "dark matter" in the universe. The signature of this dark matter is apparent in the galactic rotational curves and in the relation between masses of the supermassive black hole in the galactic center and the host galaxy. The suggested model of the electron possesses oscillation features with anomalous magnetic moment and embedded signatures of the Compton wavelength and the fine-structure constant. The analysis of the interactions between the oscillating electron and the nodes of the vacuum grid structure allows us to obtain physical meaning for some fundamental constants.

Key words: physical vacuum, structure of the electron, fine-structure constant, Compton wavelength, anomalous magnetic moment, dark matter, Planck frequency, unified theories

1. INTRODUCTION

"Dark matter" is a hot topic in cosmology today. Currently it is accepted that dark matter predominates visible matter in the universe. In recent years it has been found that most galaxies contain at their center a supermassive black hole of the order of a billion solar masses. A surprisingly strong relation has been found between the mass of the supermassive black hole and the total mass of the whole galaxy, so they are in a kind of balance.[1] Another peculiar fact of the existence of hidden matter comes from the rotational curves of the galaxies. One of the largest rotation curve databases of spiral galaxies clearly shows that dark matter is more the rule than the exception.[2] It stands to reason to raise the question, "Isn't dark matter a hidden type of matter around us and even 'within us'"? This idea further leads to the conclusion that the currently adopted concept of the physical vacuum may not be correct. This required an extensive study of some features of the physical vacuum, such as zero-point energy (ZPE), quantum fluctuations, vacuum polarization, Planck's length and frequency, and so on. In this aspect, the theoretical articles provided by T.H. Boyer,[3] H.E. Puthoff,[4–6] H.E. Puthoff et al.,[7] and B. Haisch et al.[8] appear quite useful. F.M. Meno[9] envisions hypothetical three-dimensional nonspherical particles called gyrons possessing a gyroscopic effect. He associates Planck's length and mass with some of the gyron's parameters, although he does not suggest a detailed physical model of this gyron and does not envision a possible organization of the gyrons into stable structures. The articles "Experimental evidence that the gravitational constant varies with the orientation" by M.L. Gershteyn et al.[10] and "Speed of gravity revisited" by M. Ibison et al.[11] lead to the idea that Newton's law of gravitation might be derivable instead of postulated. This idea obtained some theoretical treatment by H.E. Puthoff,[4] who derived Newton's law of gravitation starting from Planck's frequency ω_{PL} and using a hypothesis of Sakharov:

$$\omega_{PL} = \left(\frac{2\pi c^5}{hG} \right)^{1/2}, \quad (1)$$

where c is the velocity of light, h is Planck's constant, and G is the gravitational constant.

Here we may express an idea about the existence of some hypothetical structure in the microscale range, related in some way to ω_{PL}. This could be regarded as a further development of the concept of string theories, which assume the existence of some hypothetical string-like objects (open or closed loops) in a microscale range possessing a finite length but zero thickness. What could be the results if these hypothetical extended objects possessed a finite width, while their dimensions were far beyond the observational limit? In this case these strings should be regarded as material objects in a three-dimensional space and they might be organized in structures. It stands to reason that we are able to observe enormously large structures in the macroscale range of the universe, but structures may also exist in the microscale range.[12]

One additional consideration that Newton's law of gravitation might be derivable from a more fundamental one comes from its comparison with the law of optical radiation. In its simplest form, when the surfaces of two areas A_1 and A_2 are parallel to each other, the irradiation flux Φ is given by $\Phi = LA_1A_2/r^2$, where L is the emitted radiance and r is the distance between the two surfaces (visible in the subtended angle). If the two bodies are parallel disks, the radiation law depends only on the visible surfaces but not on the disk thickness. At the same time, Newton's gravitational law depends on the thickness or the bulk matter of the bodies. But why do they have one and the same dependence on the distance? It seems that Newton's gravitational mass could have some dependence on the area of the closed surface of some unknown real structure on which some hypothetical substance may exert pressure.

The above-mentioned citations and logical considerations were helpful in the search for an appropriate model of the alternative vacuum concept. An idea was born that Planck's frequency could be a parameter of some intrinsic type of matter involved in some unknown subelementary particles from which both the vacuum structure and the elementary particles are built. These hypothetical subelementary particles may possess enormous mass density and may interact in a classical void space. Their gravitational interactions, however, may be distinguished from Newton's gravitation by the degree of proportionality to the distance. In this aspect we refer to this type of gravitational interaction as intrinsic gravitation (IG). The hypothetical subelementary particles, for instance, may form stable structures if their IG in a classical void space is inversely proportional to the cube of the distance. In this way they may form a stable spatial grid. *At the same time, Newton's gravitation acting between the elementary particles and their formations (atomic nuclei, atoms, molecules) could be a result of the IG field propagation through the interconnected elements of the spatial grid.* The IG gravitation, however, may leak at some close distance between atoms and molecules (some types of van der Waals forces) or well-polished solid objects (Casimir forces).

2. BRIEF INTRODUCTION TO THE CONCEPT OF THE BSM HYPOTHESIS

The above-presented considerations serve as a starting point for the development of a hypothesis called basic structures of matter (BSM),[13],[1] associated with the class of unified theories. According to the BSM concept,[14] the IG force F_{IG} between two objects comprising the same type of intrinsic matter put in a classical void space is proportional to the product of their intrinsic masses and the intrinsic gravitational constant and inversely proportional to the cube of the distance,

$$F_{IG} = G_0 \frac{m_{01} m_{02}}{r^3}, \quad (2)$$

where G_0 is the IG constant, m_{01} and m_{02} are intrinsic masses, and r is the distance.

It is assumed that the space known as a physical vacuum possesses a underlying grid structure formed of two types of subelementary particles arranged in nodes. These two subelementary particles are built respectively by two types of intrinsic matter with different density. They both have the shape of hexagonal prisms with length-to-diameter ratio >1, while the dimensional ratio between both prisms is 2:3. They also possess a similar internal structure with twisted component, but left- and right-handed, respectively. Prisms of the same type (intrinsic matter and handedness) are attracted in a pure void space by forces according to the above-defined IG law. The attraction forces between the different types of prisms, however, are smaller and depend on the node distance, and they may convert to repulsion at some critical value of this distance. Additionally, the prisms of both types pos-

sess IG anisotropy along their axis with a left- and right-twisting component, respectively, defined by their lower-level structure. For this reason they are called twisted prisms, although they are not externally twisted. The formation of these subelementary particles is possible from much simpler spherical particles, following pure geometrical principles and preservation of the integrity of the lower-level structures in the upper-level structures. A hypothetical scenario for this is provided in Chapter 12 of BSM. According to the BSM concept, the two types of prisms build the underlying structure of the physical vacuum and the elementary particles as well. The structural integrity in both cases is assured by the IG law, defined by (2). The elementary component of the vacuum structure is a node called a cosmic lattice (CL) node. The CL node is formed of four prisms of the same type held by IG forces in positions like the four axes in a tetrahedron, but the connected prisms have some limited freedom of angular deviation. The vacuum structure is formed by alternately arranged nodes of both types with some gaps between the prisms of the neighboring nodes. The spatial CL structure is similar to the atomic lattice in a diamond. It is assumed that this structure fills the volume of the visible universe, so the space in BSM is referred to as a CL space. The elementary particles are built by the same prisms, but arranged in a configuration of helical structures inside of which a different type of spatial structure (internal lattice) from the same prisms exists. The internal lattice, however, is denser than the CL structure, so the latter could not penetrate the internal lattice. Therefore the CL space should exert a pressure on the internal lattice of the particle. The pressure parameter of the CL space leads to the derivation of a mass equation in BSM (Chapter 3). It is estimated that the node distance is of the order of 10^{-20} (m), while the overall size of any elementary particle is larger by a few orders. At the same time, the density of the intrinsic matter from which the prisms are built is many orders larger than the average density of any elementary particles. In these conditions the CL space is able to carry the elementary particles, while an accumulation of these particles in a closed volume may influence but very weakly the node distance of the CL space in close proximity (a large mass accumulation may distort slightly the node distance in the surrounding space, leading to a space curvature according to general relativity).

One specific feature of the CL space is the ability of the CL nodes to be displaced by the denser internal lattice of the moving elementary particles (every particle is in motion due to the galactic rotation). This effect involves a disconnection, a displacement with simultaneous folding of the CL node, and returning, unfolding, and reconnecting to the previous position of the CL structure. The connection energy during the displacement is transferred to kinetic energy. This unique feature does not have a counterpart in any concept of ether or ideal fluid. The folding properties of the CL nodes are also closely related to the inertial properties of the atomic matter in CL space and play a role in the equivalence between the gravitational and inertial mass.

Analyzing the dynamics and mutual interactions of the CL nodes, it is possible to associate some of their features with known physical parameters and constants, such as the ZPE of the vacuum, the velocity of light, the Compton frequency (or wavelength), and the permeability and permittivity of free space. Figure 1 illustrates the geometry of a single CL node in a position of geometrical equilibrium. The four prisms are held by IG forces defined by (2).

The CL node is characterized by two sets of axes: one set of four axes along any one of the prisms, called the *abcd* axes, and another set of three orthogonal axes, called the *xyz* axes. In a geometrical equilibrium the angle between any two of the *abcd* axes is 109.5°. The external tips of the prisms in a geometrical equilibrium define the apex points of a tetrahedron. The *xyz* axes pass through the middle of every two opposite edges of the tetrahedron. At the same time, the orthogonal *xyz* axes of the neighboring CL nodes are commonly aligned. This arrangement assures complex individual oscillations of the CL node, from one side, and strong interactions between the neighboring nodes, from the other. The dynamics and interactions are both governed by the IG law acting between the two intrinsic matter substances of the prisms and the time constant for this matter.

The dynamical behavior of the CL node is studied by estimating the shape of the return forces (under the condition of IG law) acting on the CL node deviated from the central position and keeping in mind that the node geometry is flexible. To simplify the analysis the neighboring four CL nodes are considered stationary, while their interconnecting prisms are always aligned to the CL node under consideration (for details see the BSM monograph, *http://www.helical-structures.org/Chapters/*BSM_appendix2-1.pdf). This also means that the IG interactions propagate faster than the oscillation period of the CL node. The shapes of the return forces along any one of the *xyz* and *abcd* axes are shown respectively in Fig. 2a and b.

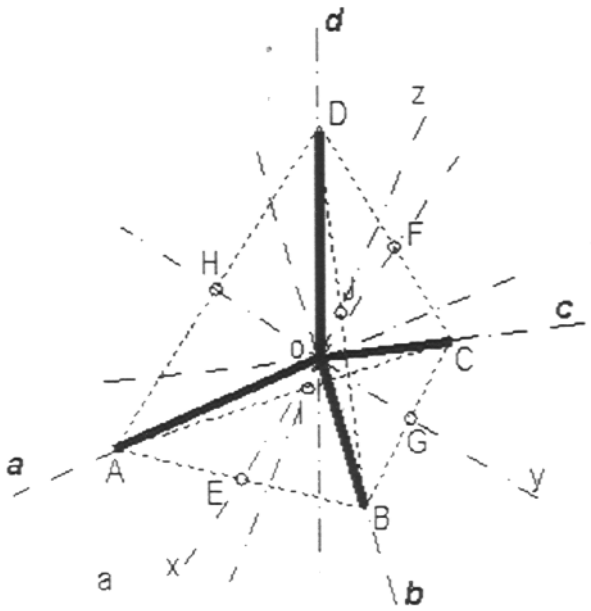

Figure 1. CL node formed of four prisms shown by thick black lines.

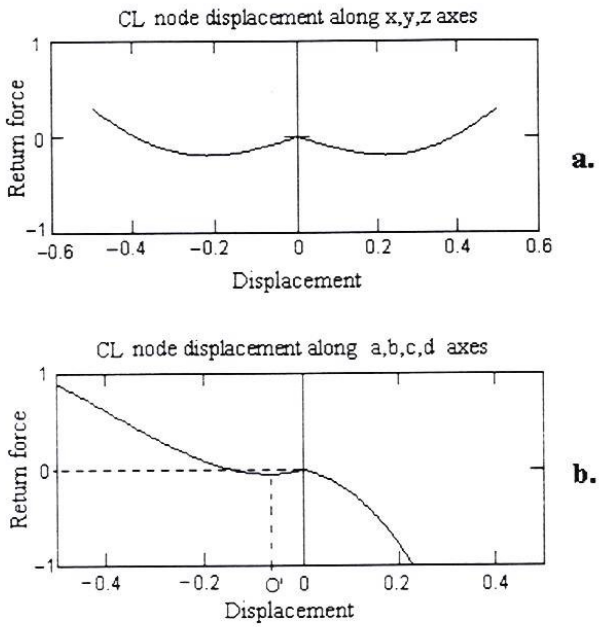

Figure 2. Return forces versus displacement of the CL node along one of the *xyz* axes (a) and *abcd* axes (b). Both scales are in relative units.

Two symmetrical minima appear along any one of the *xyz* axes and one minimum appears along the positive direction of any one of the *abcd* axes. From the point of view of CL node dynamics, they could be associated with energy wells, responsible for the ZPE of the vacuum.

The shape and the different stiffness of the return forces along the *xyz* and *abcd* axes indicate that the CL node will possess a complex type of oscillations in which two types of cycles are identifiable: a proper resonance cycle and a spatial precession momentum (SPM) cycle (the latter is described by an SPM vector). The trace of the proper resonance cycle is an approximately flat but open curve with four bumps, as shown in Fig. 3.

The bumps of the trace curve centered on the two orthogonal axes are caused by the different stiffness for node deviations along the *abcd* and *xyz* axes. The points A and B from the resonance cycle are pretty close but not coinciding, so the segment AB points almost at 90° with respect to the drawing plane. The lack of coincidence between any initial (A) and final (B) point for one proper resonance cycle is a result of the spatial positions of the minima of the return forces along the two sets of axes. The CL node dynamics for the proper resonance cycle could be described by a vector called a node resonance momentum (NRM) vector.

The average plane of the trace is slightly rotating with every NRM cycle, so after a large number of these cycles the node trace will pass through the same (arbitrarily selected) initial point A. This second type of cycle is called an SPM cycle. The vector describing this cycle is called an SPM vector. The number of resonance cycles in one SPM cycle, estimated in BSM, is quite large but constant (due to the mutual interactions of the oscillating CL nodes). The analysis in BSM indicates that this number is related to the magnetic permeability of free space (Section 2.11.3 in Chapter 2 of BSM).

The tip of the SPM vector for one full cycle circumscribes a closed surface with a central point of symmetry and six bumps along the *xyz* axes. This type of surface is referenced in BSM as an SPM quasisphere. It is found that, if the resonance cycle of the CL node is related to the energy wave propagation with the velocity of light, the SPM cycle should be related to a particular quantum feature of the CL space that assures the constant value of the velocity of light. This can be explained by the quantum properties of the SPM quasispheres and their mutual interactions. The velocity of light is considered as energy momentum propagation between two neighboring nodes (considering the *xyz* interconnection coordinates) for one resonance cycle of the CL node (Section 2.11 in

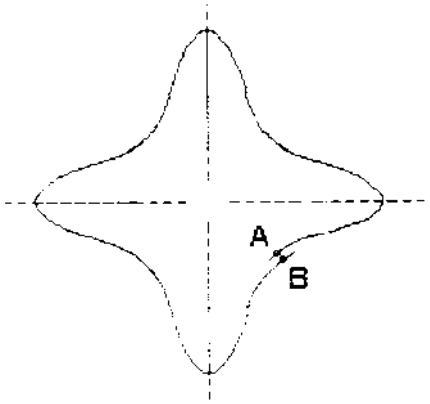

Figure 3. Trace of single proper resonance cycle of the CL node.

Chapter 2 of BSM). The frequency of the SPM cycle is associated with the well-known Compton frequency. In the absence of any electrical charge, the SPM quasisphere possesses a central point of symmetry. It is called a magnetic quasisphere (MQ) because it could provide a physical meaning for the magnetic line. The magnetic line could be formulated as *a closed loop in CL space involving only MQ types of nodes whose SPM frequencies are synchronized by a running phase propagating with the velocity of light.* This spatial configuration may exhibit features allowing the explanation of the stability and direction of the magnetic line, for example:

- The CL nodes of right-handed prisms are commonly synchronized.
- The CL nodes of left-handed prisms are commonly synchronized.
- The phase difference between the involved left- and right-handed nodes determines the direction of the magnetic line, referenced to the laboratory frame, for example, a +90° phase difference for the N-S direction and a –90° phase difference for the S-N direction.
- The involved MQ nodes may additionally have a helical arrangement along the closed loop.

The above considerations are for the permanent magnetic field. In the case of the alternative magnetic field the commonly spatially dependable synchronizations of the left- and right-handed nodes vary with time.

Aligned MQs with a spontaneous phase synchronization (with light velocity) may also exist in an open loop, but temporally. This is a normal state of the oscillating CL node when considering the mutual interactions of the neighboring CL nodes, and this effect appears to be related to the magnetic permeability of free space.

In the presence of a charge particle, the SPM quasisphere obtains a deformation as an elongation along its diameter connecting two opposite bumps, so it is called an electrical quasisphere (EQ). The shapes of MQ and EQ are shown in Fig. 4.

For simplification of analysis when studying the dynamics, the positions of the CL nodes could be considered as stationary in a laboratory frame. The electrical field could be presented as spatially oriented and synchronized EQ CL nodes. When studying the conditions of energy propagation as a wave, it is convenient to use imaginary *running CL nodes*. Then the phase propagation of the SPM vector with the speed of light through stationary positioned CL nodes can be regarded as a running SPM vector. In this manner the temporal variation of the common synchronization of the CL nodes is easily studied. The analysis in this approach leads to the unveiling of the structure of the photon. It is found that the EQ-type node possesses a larger energy than the MQ type (see Section 2.10.4.3, Chapter 2, of BSM). The photon wave-train can be presented as a complex arrangement of *running EQs* with a decreasing elongation from the central axis of the wave-train to its boundary radius, where they are converted to *running MQs*. Thus it appears that the photon wave-train possesses boundary conditions (a longstanding problem). At the same time, the running EQs are aligned in a helix with a step equal to the photon wavelength.

The analysis of the CL node dynamics as EQ and MQ types and the suggested photon wave-train structure in a normal CL space (possessing a normal ZPE) are presented in Chapter 2 of BSM. The CL space with a subnormal ZPE and the behavior of the charge particles in this case are analyzed in Chapter 4 of BSM.

The applied new approach allows us to admit that the elementary particles also possess an underlying structure built by the same subelementary particles — the two types of prisms. BSM analysis leads to a conclusion that the stable particles, such as the proton, neutron, and electron (and positron), possess stable structures with well-defined spatial geometry and denser internal lattices. They comprise complex but understandable three-dimensional helical structures whose elementary building blocks are the above-mentioned prisms, arranged in a strong particular order. The analysis provided in Chapter 8 of BSM leads

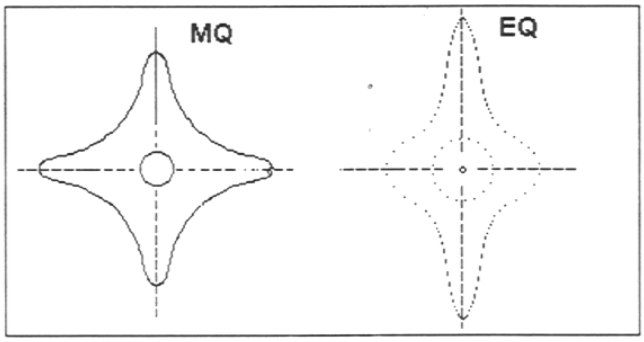

Figure 4. Shape of MQ (left) and EQ (right).

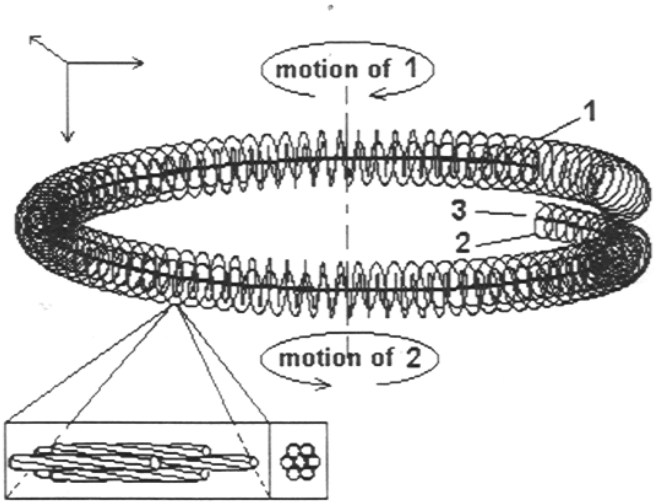

Figure 5. Oscillating electron comprises three helical structures: (1) external negative, (2) internal positive, and (3) internal negative core. The internal lattices are not shown. The expanding box in the lower left side shows an elementary node of the helical structure 1, formed of seven right-handed prisms (they are not externally twisted; the twisting is for concept visualization only).

to a conclusion that the protons and neutrons are spatially arranged in the atomic nuclei.[15] If the suggested vacuum structure is real, the interpretation of the scattering experiments should be reconsidered, because neither the vacuum structure nor the structure of the elementary particles has been taken into account so far.

3. A PHYSICAL MODEL OF THE ELECTRON BUILT ELEMENTARY PARTICLES

According to the BSM concept, the electron possesses the simplest structure among the stable elementary particles. The suggested physical model of the electron comprises three helical structures, one inside another, as illustrated in Fig. 5. The helical structure comprises a helical envelope and an internal lattice inside this envelope. All of them are built by the suggested subelementary particles (prisms). The axial section of an elementary core from any helix envelope contains seven prisms of the same type, one in the center and six on the periphery. At the same time, they are axially displaced (as shown in Fig. 5), so the helix could be considered as formed of stacked elementary cores. The two helical structures of the electron possess denser internal lattices located in the internal spaces of the helix envelopes (not shown in this figure).

The dimensions of the physical components of the electron structure are denoted as R_C, the Compton radius of the electron (known), r_e, a small electron radius, r_p, a small positron radius, and s_e, a helical step. The derivation of these dimensions is discussed later.

The electron structure shown in Fig. 5 has two internal lattices spaced inside the volume enclosed by the two helical structures. Each one is built of the same type of prisms as its envelope. The outer lattice has a larger hole in its radial section where the internal first-order helical structure oscillates. The other internal lattice has a smaller hole where the internal core oscillates.

The geometrical considerations allowing us to build the internal lattice are illustrated in Fig. 6.

Every RL node comprises six prisms of the same type. The axial section contains a number of concentric layers. Starting from the cylindrical boundary defined by the helix envelope, the most external layer is connected to the helix by IG forces, while every internal layer is connected to the neighboring external one. The thickness of every internal layer is half of the thickness of the neighboring external layer. The radially aligned prisms of the neighboring nodes are without gaps, while the gap length between the tangentially aligned prisms in the radial section varies when moving from the external to the internal radius of the layer.

When considering an open formation of helical structures, as for the electron (both ends are not connected as in a torus), the overall configuration could not be stable if the internal lattices were of rectangular type. This formation, however, can be stabilized if the internal RL structures get some twisting.

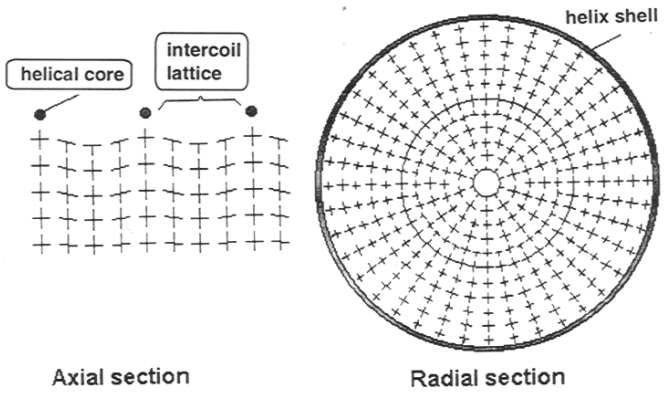

Figure 6. Configuration of the internal lattice of type RL inside the cylindrical space enveloped by the helical core, which forms the helical structure. The actual number of layers in the radial section is much larger than shown in the figure, because the prism size is a few orders smaller than the radial section diameter.

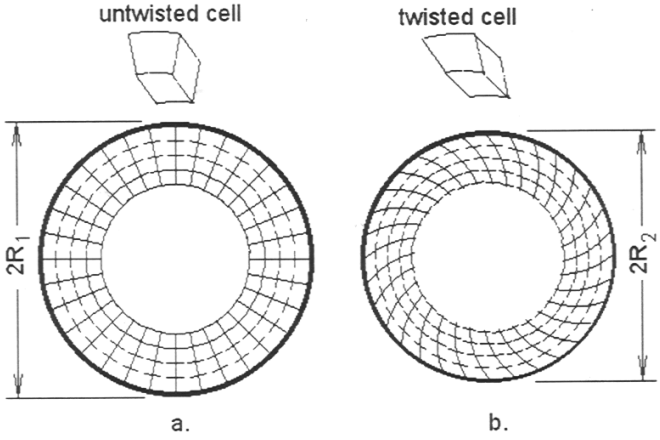

Figure 7. Radial section of untwisted (a) and twisted (b) RL structures, referred to respectively as RL and RL(T). $R_2 < R_1$.

Figure 7 illustrates the radial section of untwisted (a) and twisted (b) RL structures, referred to respectively as RL and RL(T).

The stiffness of the RL structure defined by the prism density is about 1000 times larger than the stiffness of the CL structure of the vacuum, so the volume of the RL structure is not penetrative even for folded CL nodes. Consequently, it displaces the CL structure, or, in other words, it feels a CL pressure. This is a static CL pressure.

The twisted radial strips of RL(T) modulate the dynamical properties of the CL nodes in the surrounding space, more accurately their SPM quasispheres. In this way they become EQ-type nodes arranged in line extensions from the twisted radial strips of RL(T). These spatially arranged EQ nodes form the electrical field of the charge particle — in our case the electron. This is illustrated in Fig. 8. It is evident that in a near range the electrical lines might be slightly curved, but in a far range they appear as emerging from a point.

One from each type of the prisms (for instance the right-handed) could be associated with the negative electricity and the other with the positive one, keeping in mind that the electrical charge is a property of the CL space, related to the presence of EQs, and not a property of the prism itself.

The external helical structure of the electron, referred to in BSM as an external shell, possesses an internal denser lattice (from right-handed prisms, for example). It is responsible for the creation of the EQ-type CL node as radial extensions from the RL(T).

The curved line extensions near the external electron shell are essential to the confined motion that the electron exhibits in CL space.

The internal helical structure with an internal RL(T) (from left-handed prisms) with a central core (from right-handed prisms) is an *internal positron*. When completely inside the external electron shell, it is not able to modulate the external CL space, but when it is outside it appears as a positive charge. When the internal positron oscillates inside the external electron shell, its charge only partially appears in CL space with a rate of the oscillation cycle. Due to the high oscillation frequency (discussed below), only its magnetic signature may interact with the external CL space.

Considering the oscillation properties of the suggested model of the electron, it could be regarded as a three-body system: an external helical structure with its internal lattice (external shell built of negative prisms), an internal helical structure with its internal lattice (internal shell built of positive prisms), and the central core (built of negative prisms). Both the internal helical structure and the central core oscillate in conditions of ideal bearing because their central positions are kept by the IG field and the whole structure has a complete helical symmetry with respect to the central core. In these conditions the electron structure will have two proper frequencies:

- a first proper frequency for the oscillations between the external electron shell and the internal positron,
- a second proper frequency for the oscillations between the internal positive shell and the central negative core (a proper frequency for the internal positron).

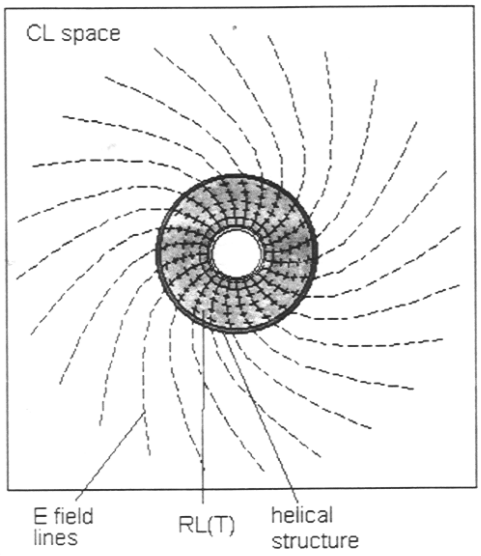

Figure 8. Proximity E-field lines (in CL space) emerging from the RL(T) structure.

From the analysis of the dynamical properties of the suggested structure it appears that the first proper frequency of the electron is equal to the SPM frequency of the CL node. This is the well-known Compton frequency.

4. QUANTUM MOTION OF THE ELECTRON AND DERIVATION OF ITS STRUCTURAL PARAMETERS

The values of the physical constants and parameters used in the presented analysis are given in Table I.

Table I: Used Fundamental Constants[16] According to CODATA 98

Constant	*Value*	*Unit*	*Name*
α	$7.297352533(27) \times 10^{-3}$		fine-structure constant
c	2.99792458×10^{8}	m/s	velocity of light
λ_C	$2.426310215 \times 10^{-12}$	m	Compton wavelength
h	$6.62606876(52) \times 10^{-34}$	J · s	Planck constant
ε_0	$8.854187817 \times 10^{-12}$	F/m	permittivity of free space
m_e	$9.10938188(72) \times 10^{-31}$	kg	electron mass
a_0	$0.5291772083(19) \times 10^{-10}$	m	Bohr radius
K_J	$483597.898(19) \times 10^{9}$	Hz/V	Josephson constant
R_∞	$1.973731568549(83) \times 10^{7}$	1/m	Rydberg constant

It is assumed and extensively discussed in the BSM hypothesis that the prisms, formed of superdense intrinsic matter, possess quite different inertial properties in a pure void space. (The very high interaction frequency of this matter may be closer to the Planck frequency and consequently it may have very small inertial properties.) It is apparent that the CL structure from its side possesses a time constant, which is obviously defined by the proper resonance frequency of the CL node.

The analysis of the motion behavior of the electron structure in CL space leads to a conclusion that it will possess a preferable type of screw-like motion. This motion in the CL space environment is possible if some CL nodes are temporally disconnected, displaced, and then returned and reconnected to the CL space.

This type of motion is referred to as confined. Two types of confined motion are identified: (1) a confined motion with optimal and suboptimal velocities, and (2) a confined motion with superoptimal velocities.

4.1 Confined Motionwith Optimal and Suboptimal Velocities

Both the CL node and the rotating electron oscillate with a Compton frequency. It is found that, when the tangential velocity of the rotating and oscillating electron is equal to the velocity of light, the phase of its first proper frequency matches the phase of the SPM vector, propagating with the velocity of light. At the same time, the internal core oscillation (with a proper frequency of three times the Compton frequency) provides a third harmonic feature for this motion. As a result, the rotating and oscillating electron exhibits a maximum interaction with the CL space — a kind of quantum interaction. The electron axial velocity for this case is $V_{ax} = \alpha c$ (corresponding to a kinetic energy of 13.6 eV). It is referred to in BSM as an *optimal confined velocity* and the motion is referred to as an *optimal confined motion*. We may consider that any point of the electron structure corresponding to a radius R (measured from the central point of the whole structure) moves with a tangential velocity equal to the speed of light (because it appears from the analysis that $r_e << R$). For this point of the structure the following relations are valid:

Peripheral velocity: c; path: $(4\pi^2R^2 + s_e^2)^{1/2}$;
Axial velocity: V_{ax}; path: s_e.

Then the axial velocity is

$$V_{ax} = \frac{cs_e}{(4\pi^2R^2 + s_e^2)^{1/2}}. \qquad (3)$$

From the Bohr model of hydrogen we know that the kinetic energy of 13.6 eV corresponds to an electron motion in orbit of radius a_0, with a velocity given by

$$V_{ax} = \frac{q_0^2}{2h\varepsilon_0} = \alpha c = 2.187691\times10^6 \text{ m/s}, \quad (4)$$

where q_0 is the elementary charge, h is Planck's constant, ε_0 is the permittivity of the vacuum, α is the fine-structure constant, and c is the velocity of light.

Therefore we arrive at the following two conclusions:

1. The screw-like motion of the suggested electron model with a tangential velocity equal to the speed of light is energetically equivalent to an electron motion in a circular orbit of radius a_0, according to the Bohr model of hydrogen.
2. The fine-structure constant appears to be a ratio between the axial and tangential velocity of the electron, when it performs an optimal confined motion.

Combining (3) and (4), we obtain a step-to-radius ratio of the electron:

$$\frac{R}{s_e} = \frac{(1-\alpha^2)^{1/2}}{2\pi\alpha} = 21.809. \quad (5)$$

Now let us assume that the first proper frequency of the electron is equal to the Compton frequency (a parameter of the CL node) and the electron structure makes one full rotation for duration equal to the Compton time t_C, which is the reciprocal of the Compton frequency:

$$\text{path} = 2\pi R = ct_C = c\left(\frac{1}{\nu_C}\right). \quad (6)$$

Solving the system of (5) and (6), we get the values of R and s_e.

$R = 3.86159 \times 10^{-13}$ (m): the large radius of the electron;
$s_e = 1.77061 \times 10^{-14}$ (m): the helical step.

It is not a surprise that the obtained value for R is exactly the Compton radius R_C, which was experimentally determined by Arthur Compton. Substituting R with R_C in (5) and having in mind that $2\pi R_C = \lambda_C$, we obtain an expression for the helical step s_e:

$$s_e = \frac{\alpha\lambda_C}{(1-\alpha^2)^{1/2}}. \quad (7)$$

The Compton wavelength λ_C is related to the Compton frequency ν_C by the simple expression $\lambda_C = c/\nu_C$. The velocity of light is related to the resonance frequency of the CL node, while the Compton frequency is the SPM frequency. Then, from (7), we have the following conclusion: *The suggested model of the electron is characterized by two embedded fundamental constants: the fine-structure constant and the Compton wavelength.*

From a number of considerations given in Sections 3.6 and 3.11.2 of Chapter 3 in BSM it appears that $s_e \approx 2r_e$, and it is assumed that this relation is more accurately expressed by the gyromagnetic factor g_e, which is experimentally determined with high accuracy:

$$s_e = g_e r_e = 2.002319 r_e. \quad (8)$$

From the analysis of the fractional quantum hall experiments in Chapter 4 of BSM, it is found that $r_p/r_e = 2/3$. Then all geometrical parameters of the electron are determined.

At the optimal confined motion with a velocity $V_{ax} = \alpha c$ (13.6 eV) the quantum interaction of the oscillating electron with the oscillating CL nodes is strongest. It is apparent that the electron may also perform a screw-like motion with smaller velocities. Let us consider these velocities for which the electron makes a complete rotation for a whole number of first proper frequency cycles. This set of axial velocities could be expressed by (9), where n is an integer:

$$V_{ax} = \frac{\alpha c}{n}. \quad (9)$$

If we use the kinetic energy of the electron instead of its axial velocity, we have

$$E = \frac{0.5h\nu_C\alpha^2}{n^2} \text{ (J)}, \quad (10)$$

$$E_{ev} = \frac{0.5h\nu_C\alpha^2}{n^2 q_0} \text{ (eV)}, \quad (11)$$

where h is Planck's constant, ν_C is the Compton frequency, and q_0 is the electron charge

The integer n is called in BSM a *subharmonic number*, in order to denote the quantum motion conditions of the electron. A quantum motion with a first harmonic velocity corresponds to 13.6 eV, with a second subharmonic to 3.4 eV, with a third subharmonic to 1.51 eV, and so on. It is evident that the introduced subharmonic number n matches the quantum number of the electron orbit in the Bohr atomic model. At the same time, it is informative about the rotational spin motion of the oscillating electron if referencing its rotation cycle to the SPM cycle of the CL space:

13.6 eV: 1 rotation cycle per SPM cycle (an optimal confined motion);
3.4 eV: 1/2 rotation cycle per SPM cycle;
1.51 eV: 1/3 rotation cycle per SPM cycle;
0.85 eV: 1/4 rotation cycle per SPM cycle;
SPM cycle period = Compton time.

By analyzing the confined motion of the electron we can get some insight into its influence on the SPM quasispheres surrounding its trace of motion. It is found that the surrounding EQs of the moving electron will cause the formation of a spatially ordered synchronization of the surrounding MQs in closed loops, i.e., the creation of magnetic lines. In this aspect it is useful to analyze the magnetic radius of the electron at different subharmonic numbers. We may consider that the rotating IG field of the internal lattice of the electron helical structure (that modulates the CL space) cannot exceed the velocity of light. Then the magnetic influence could be extended up to some limited range and we may regard it as a magnetic radius.

The magnetic radius of an electron with a kinetic energy of 13.6 eV is obtained from the analysis of the quantum magnetic field Φ_0 (see Section 3.11 in Chapter 3 of BSM): $\Phi_0 = h/q_0$, where h is Planck's constant and q_0 is the electrical charge. The obtained value of r_{mb} for 13.6 eV is almost equal to R_C, but slightly larger due to the finite thickness of the electron helical structure. The electron model also gives some insight into its magnetic moment. The magnetic moment of the electron is considered anomalous because it is distinguished from the Bohr definition of magnetic moment by the term $\alpha/(2\pi)$:

$$\mu_e = \frac{q_0 h}{4\pi m_e}\left(1+\frac{\alpha}{2\pi}\right), \qquad (12)$$

where m_e is the mass of the electron.

The anomalous term in (12) appears because the overall shape of the electron is not a torus but a single coil, possessing a helical step. Having this shape the electron is able to advance by the size of a full step, s_e, for one revolution, so this feature contributes to the anomalous term $\alpha/(2\pi)$. This feature is not taken into account when the magnetic moment is defined from the considerations of the Bohr atom. The magnetic moment is discussed in detail in Section 3.11, Chapter 3, of BSM.

4.2 An Electron Motion with Superoptimal Velocities

The optimal confined motion of the electron (axial velocity of $V_{ax} = \alpha c = 2.18769 \times 10^6$ (m/s)) could be regarded as an ideal case of the screw-like motion. In this motion the rim of the electron structure slides as in a thread, and the oscillation of the central core (with a proper frequency three times higher than the first proper frequency) provides a hummer-drill effect, enhancing the interaction with the stationary CL nodes. Keeping in mind that the phase of the SPM frequency propagates with the speed of light, it is evident that the screwing electron is moving as in a lubricated thread. At this quantum velocity the electron exhibits a maximum quantum interaction with the CL space. For larger velocities (or energies larger than 13.6 eV) the motion is still confined, but the screwing is not as in a thread (because no point of the electron structure could exceed the velocity of light, which is restricted by the proper resonance frequency of the CL node). Therefore we may expect a decrease in the quantum efficiency for these velocities. This is discussed in Section 3.11.A.1, Chapter 3, of BSM, where an expression for the quantum efficiency is derived. The obtained expression appears to be a reciprocal function of the relativistic gamma factor. This is in agreement with the mass increase of the electron at relativistic velocities.

5. RYDBERG CONSTANT AS A SIGNATURE OF THE OPTIMAL CONFINED MOTION OF THE ELECTRON

Let us consider a quantum motion of the electron (13.6 eV) with an optimal confined velocity ($n = 1$, n is a subharmonic number). The electron energy for $n = 1$, according to (10), is

$$E = 0.5 h\nu_C \alpha^2 \text{ (J)}. \qquad (13)$$

The energy of the 13.6-eV photon is expressed by

$$E = h\nu_C = hc\sigma \text{ (J)}, \qquad (14)$$

where $\sigma = 1/\lambda_C$ is the wave-number, ν_C is the Compton frequency, and c is the velocity of light.

Equations (13) and (14) provide one and the same energy (13.6 eV). Solving this system for σ, we get the Rydberg constant in wave-numbers:

$$\sigma = R_\infty = \frac{\nu_C \alpha^2}{2c} = 1.097373156 \times 10^7 \text{ (1/m)}. \quad (15)$$

The suggested model of the electron contains an embedded fine-structure constant, as seen from (7). Additional analysis in BSM (Section 2.9.6.B of Chapter 2 and Section 9.7.5 of Chapter 9, from the first edition of BSM) indicates that the fine-structure constant is in fact an intrinsic parameter of the CL space. The Compton frequency is also a CL space parameter characterizing the CL node dynamics. Then from (15) it follows that the Rydberg constant is also a CL space parameter. The way it was derived indicates that *the Rydberg constant appears as a characteristic feature of the quantum motion of the electron with an optimal confined velocity.*

6. QUANTUM MOTION OF THE ELECTRON IN A CLOSED-LOOP TRAJECTORY

The orbital motion of the electron in atoms could be regarded as a motion in a closed loop, whose trajectory follows the equipotential surface of an electrical field defined by one or more positive charges.

Let us consider a repetitive motion in a closed loop. The modulation properties of the internal RL(T) lattice in a repetitive motion may cause distortion of the MQs (which is a normal state of the SPM vector), converting them into EQs. This will affect the orbital conditions defined by the proximity field of the proton. Let us assume that the orbital motion of the oscillating electron tends to adjust itself to this change by exchanging some reactive energy with the CL space, which is hidden from the external observer. Then we may analyze the phase repetitions of the two proper frequencies of the electron and the conditions of their match to the phase of the SPM frequency of the CL nodes. In this way we may assume that the stability of a repetitive motion in this loop will depend on the phase repetition for both the first and the second proper frequencies of the electron.

We will try to find the smallest path length at which the quantum loop conditions for an electron moving with a velocity corresponding to $n = 1$ (13.6 eV) is fulfilled. *Initially we will ignore the relativistic effect for simplicity.* It is reasonable to look for a path length defined by some CL space parameter. One such parameter is the Compton wavelength λ_C, related to the Compton frequency ν_C by the simple expression $\lambda_C = c/\nu_C$. For one orbital cycle in a closed loop with length λ_C, the number of turns (electron structure rotations) N_T is

$$N_T = \frac{\lambda_C}{s_e} = 137.03235. \quad (16)$$

The value of N_T could be regarded as a condition for a phase repetition for two consecutive passages through a chosen point in the loop, keeping in mind a confined (screw-like) motion of the electron. The trace length of $\lambda_C = 2.4263 \times 10^{-12}$ (m), however, is quite small when compared to the Bohr orbit length of $2\pi a_0 = 3.325 \times 10^{-10}$ (m). Therefore we may look for phase repetition conditions at a larger loop length. From (16) we see that N_T is close to $1/\alpha = 137.036$ and this seems not accidental. Then we may substitute N_T in (16) by $1/\alpha$ and multiply the result by λ_C. The latter is a CL space parameter from one side (a length of SPM phase propagation for one SPM cycle), and from the other it is the circumference length of the electron structure. In this case we obtain

$$N_T \lambda_C = \frac{1}{\alpha} \lambda_C = 3.24918460 \times 10^{-10} \text{ (m)}. \quad (17)$$

We see that the obtained value of (17) having a dimension of length is equal to the Bohr orbit length given by CODATA 98 (see Table II) up to the ninth significant digit:

$$2\pi a_0 = 3.24918460 \times 10^{-10} \text{ (m) (CODATA 98)}, \quad (18)$$

where $a_0 = 0.5291772083 \times 10^{-10}$ (m) is the radius of the Bohr atomic model of hydrogen.

The expression (17) is not new. The important fact, however, is the way it is derived using the suggested physical model of the electron. The obtained loop length appears equal to the orbit length of the Bohr atom, defined by the Bohr atomic radius a_0. The latter is one of the basic parameters used in quantum mechanics. From the BSM point of view, however, the physical meaning of this parameter appears different.

According to the BSM concept, the well-known parameter a_0, used as a radius in the Bohr model, appears defined only by the quantum motion conditions of the electron moving in a closed loop with an opti-

mal confined velocity corresponding to an electron energy of 13.6 eV. Then the main characteristic parameter of the quantum loop is not its shape, but its length.

The identity of (17) and (18) also indicates that *the signature of the fine-structure constant is embedded in the quantum loop.*

Now we may use the new obtained meaning of the quantum loop associated with the Bohr orbit, and more specifically the orbital length $2\pi a_0$. For a motion with an optimal confined velocity the number of electron turns in the quantum orbit is equal to the orbital length divided by the helix step (s_e):

$$\frac{2\pi a_0}{s_e} = \frac{\lambda_C}{\alpha s_e} = 18778.365 \text{ turns.} \qquad (19)$$

Let us find at what number of complete orbital cycles (for orbit length of $2\pi a_0$) the phase repetition of the first and second proper frequencies of the electron is satisfied (in other words the smallest number of orbital cycles containing a whole number of two frequency cycles). The analysis of the confined motion of the electron in Chapters 3 and 4 of BSM indicates that its secondary proper frequency is three times higher than the first one (the first one is equal to the Compton frequency). Equation (19) shows that the residual number of first proper frequency cycles is close to 1/3. If we assume that it is exactly 1/3 (due to a not very accurate determination of the involved physical parameters), then the condition for phase repetition of both frequency cycles will be met for three orbital cycles. The whole number of turns then should be $3\lambda_C/(\alpha s)_e$. Substituting s_e by its expression given by (7), we get

$$\frac{3(1-\alpha^2)^{1/2}}{\alpha^2}. \qquad (20)$$

We have ignored so far the relativistic correction, but for accurate estimation it should be taken into account. The relativistic gamma factor for the electron velocity of $V_{ax} = \alpha c$ is $\gamma = (1 - \alpha^2)^{-1/2}$. Multiplying the above expression by the obtained gamma factor, we get

$$\frac{3}{\alpha^2} = \text{integer.} \qquad (21)$$

The validity of (20) and (21) could be tested by the following simple procedure: calculate these expressions by using the best experimental value of α, round the result to the closest integer (satisfying the condition for two consecutive phase repetitions), and recalculate the corresponding value of α. The rounded integer (a whole number of turns) could be correct only if the recalculated value is in the range of the accuracy of the experimentally determined α. Let us use the recommended value of experimentally measured α according to CODATA 98:

$$\alpha = 7.297352533(27)\times 10^{-3} \text{ (CODATA 98),}^{(16)} \qquad (22)$$

where the uncertainty error is denoted by the digits in brackets.

The calculated values of α from (20) and (21) exceed by quite a bit the uncertainty value of experimentally determined α given by (22). Consequently, the condition for phase repetitions of the two proper frequencies is not fulfilled for three orbital cycles with total trace length of $3 \times 2\pi a_0$. Therefore we may search for the next smallest number of orbital cycles in which the phase repetition conditions are satisfied. It stands to reason that the approximate value of the orbital cycles could be about 137 ($1/\alpha$). Then, if we are not considering relativistic correction, the corresponding number of electron turns is $(1 - \alpha^2)/\alpha^3$. When applying a relativistic correction (multiplying by the above-estimated gamma factor for the kinetic energy of 13.6 eV), the number of electron turns becomes $1/\alpha^3$. The phase repetition conditions will be satisfied if this number is integer: $1/\alpha^3$ = integer.

Substituting α by its value from CODATA 98 (22), we get $1/\alpha^3 = 2573380.57$.

It is interesting to note that the closest integer value of 2573380 is obtained by Michael Wales, using a completely different method for analysis of the electron behavior. (See Michael Wales's book *Quantum Theory: Alternative Perspectives*.[17])

We may use one additional consideration to validate the above-obtained number. The number of turns multiplied by the time for one turn (the Compton time) will give the total time on the orbit (or the lifetime of the excited state, according to the quantum mechanics terminology). If we accept that the total number of turns is 2573380, then we obtain a lifetime of 2.0827×10^{-14} (s), which appears to be at least two orders smaller than the estimated lifetime for some excited states of atomic hydrogen.

Following the above analysis, we may check for phase repetition at $1/\alpha^4$ turns. The participation of α at a power of four is in agreement also with the fol-

lowing consideration: In the analysis of the vibrational mode of molecular hydrogen, an excellent match between the developed model and observed spectra (Section 9.7.5 in Chapter 9 of BSM) is obtained if the fine-structure constant participates at a power of four. In this case we may accept that the phase repetition condition is satisfied for a number of turns given by the closest integer in (23):

$$\frac{1}{\alpha^4} = \text{integer}. \qquad (23)$$

Using the CODATA value of α, we obtain $1/\alpha^4$ = 352645779.39. Rounding to the closest integer, we obtain an expression for the theoretical value of α (if its experimental estimation is accurate enough):

$$\alpha = (352645779)^{-1/4} = 7.2973525298\times10^{-3}. \qquad (24)$$

The small difference of the theoretically obtained value of α from the experimental one could be caused by experimental error. One of the methods for accurate experimental estimation of α is based on the measurement of the Josephson constant K_J. Its connection to α is given by the expression

$$K_J = \frac{2}{c}\left(\frac{2\alpha}{\mu_0 m_e \lambda_C}\right)^{1/2}, \qquad (25)$$

where μ_0 is the permeability of vacuum, m_e is the electron mass, c is the velocity of light, and λ_C is the Compton wavelength.

The accuracy of α according to this method depends mostly on the accuracy of the Josephson constant measurement, because all other parameters are accurately known. The recommended value for this constant according to CODATA 98 is K_J = 483597.898(19) × 10^9 (Hz/V). If we replace α in (25) with the value given by (22), we will obtain the value of K_J that is in the uncertainty range given by CODATA 98.

The conclusion that the orbital duration may depend only on α is reinforced by the consideration that the Compton wavelength λ_C was initially involved in the analysis ((15), (17), (19)), but it disappeared in the derived (23). Consequently, the phase repetition condition is satisfied not only for the two proper frequencies of the electron but also for the SPM frequency of the CL nodes included in the quantum orbit (λ_C is propagated with a speed of light phase of the SPM vector for one SPM cycle of the CL node (SPM frequency = Compton frequency)).

Table II shows the quantum motion parameters of the electron in a quantum loop for velocities corresponding to different subharmonic numbers. n is the subharmonic number, E is the electron energy, V_{ax} is the axial velocity, V_t is the tangential velocity of the rotating electron structure, r_{mb} is the equivalent magnetic radius of the electron limited by the speed of light modulation of the CL nodes from the rotating electron structure, c is the velocity of light, R_C is the Compton radius, a_0 is the Bohr radius, l_{ql} is the trace length for motion in a closed loop (single quantum loop), and L_q is the length of a quantum loop if its shape is a Hippoped curve with a parameter $a = 3^{1/2}$ (close to the shape of a figure 8).

Table II: Quantum Motion Parameters of the Electron in a Quantum Loop

n	E (eV)	V_{ax}	V_t	r_{mb}	l_{ql}	L_q (Å)
1	13.6	αc	c	~R_C	$2\pi a_0$	1.3626
2	3.4	$\alpha c/2$	$c/2$	$2R_C$	$2\pi a_0/2$	0.6813
3	1.51	$\alpha c/3$	$c/3$	$3R_C$	$2\pi a_0/3$	0.4542
4	0.85	$\alpha c/4$	$c/4$	$4R_C$	$2\pi a_0/4$	0.3406
5	0.544	$\alpha c/5$	$c/5$	$5R_C$	$2\pi a_0/5$	0.2725

The introduced parameter *subharmonic number* shows the rotational rate of the whole electron structure.

7. QUANTUM ORBITS

It is apparent from the provided analysis that a stable quantum loop is defined by the repeatable motion of an oscillating electron. The shape of this loop, however, is determined by external conditions. These conditions may exist in the following two cases:

- a quantum loop obtained between particles with equal but opposite charges and equal mass, as in the case of the positronium (see Chapter 3 of BSM);
- a quantum loop obtained between oppositely charged particles with different masses (a hydrogen atom as the most simple case and other atoms and ions as more complex cases).

In both options the quantum loops are repeatable and we may call them *quantum orbits*. A single quantum orbit could contain one or a few serially connected quantum loops (in both cases the condition for phase repetition is preserved). It is obvious that the shape of the quantum orbit is defined by the proximity field configuration of the proton (or protons). The vacuum

space concept of BSM allows the unveiling of not only the electron structure but also the physical shape of the proton with its proximity electrical field (Chapters 6 and 7 of BSM). The shape of any possible quantum orbit is strictly defined by the geometrical parameters of the proton.

Let us consider now the induced magnetic field of the electron motion in a quantum orbit by using the electron magnetic radius. The magnetic radius of the electron moving with different subharmonic numbers n is analyzed in Section 3.1, Chapter 3, of BSM. Its value for $n = 1$ (a kinetic energy of 13.6 eV) matches the estimated magnetic radius corresponding to the magnetic moment of the electron. For larger numbers (decreased electron energy), however, the magnetic radius shows an increase. The physical explanation by BSM is that at decreased rate of electron rotation the IG field of the twisted internal RL structure is able to modulate the surrounding CL space up to a larger radius until the rotating modulation of the circumference reaches the speed of light. Keeping in mind that the circumference of the electron is equal to the Compton wavelength (with a first-order approximation), the circumference of the boundary (defined by the rotation rate) should be a whole number of Compton wavelengths. Then the integer number of the Compton wavelengths corresponds to the integer subharmonic number. In this case the orbiting electron with optimal or suboptimal velocity cannot cause an external magnetic field beyond some distance from the nucleus. This provides boundary conditions for the atoms if we accept that in any quantum orbit the electron is moving with optimal or suboptimal confined velocity (integer subharmonic number). Here we must open a bracket that the higher energy levels in heavier elements come not from a larger electron velocity but from the shrunk CL space affected by the accumulated protons and neutrons. This CL space domain is pumped to larger energy levels in comparison to the CL space surrounding the hydrogen atom.

The existence of the IG law changes significantly the picture of the orbiting electron in a proximity field of the proton. In Chapter 7 of BSM an analysis of the Balmer model of the hydrogen atom is developed based on the BSM concept of the electron and proton and the IG law's influence on the orbital electron motion in the proximity of the proton. It appears that the limiting orbit has a length of $2\pi a_0$, while all other quantum orbits are inferior. This conclusion is valid not only for the Balmer series in hydrogen but also for all possible quantum orbits in different atoms, if they are able to provide line spectra. Therefore the obtained physical model of hydrogen sheds some light on the solution of *the boundary conditions problem of electron orbits in atoms.*

8. DURATION OF A STABLE ORBIT (LIFETIME OF EXCITED STATE)

The following analysis could be valid only for hydrogen, where the influence of the proton mass on the surrounding CL space appears to be negligible.

Keeping in mind the screw-like confined motion, the axial and tangential velocities will be inversely proportional to the subharmonic number. Then the condition for phase repetitions for a motion with a subharmonic number n will be satisfied for an n times smaller number of electron turns, or the quantum orbit will be n times smaller. It is reasonable to consider that the first and second proper frequencies of the electron are stable and not dependent on the subharmonic numbers. Then to estimate the duration of the orbit (the lifetime of the excited state) it is more convenient to use the number of cycles of the first proper frequency of the electron. It is equal to the number of electron turns for $n = 1$. In this way we arrive at the following conclusion:

a) If conditions for a stable quantum orbit are defined only by the phase repetition conditions and the whole number of Compton wavelengths, the duration (lifetime) of the orbiting electron does not depend on the subharmonic number of its motion.
b) If (a) is valid, the lifetime of the excited state will be equal to the product of the total number of first proper frequency electron cycles (according to (23)) and the Compton time (the time for one electron cycle with the first proper frequency).

According to condition (b), the theoretical lifetime for an excited state of hydrogen is

$$\tau = \frac{t_C}{\alpha^4} = \frac{\lambda_C}{c\alpha^4} = 2.85407\times10^{-12} \text{ (s)}, \qquad (26)$$

where t_C is the Compton time.

Note: The obtained equation (26) does not take into account the possible modification of the surrounding space in close proximity to the proton. This modification (a slight shrinkage, or a space curvature) may cause aliasing for the phase repetition conditions due to affected SPM frequency and Compton wavelength, while the first and second proper frequencies of the

electron are obviously stable. For heavier atoms this modification may appear much stronger. For elements with more than one electron the mutual orbital interactions may also lead to an increase in the real lifetime.

The physical constants used in this article are given in Table I above.

9. CONCLUSIONS AND COMMENTS

According to the BSM hypothesis, the physical model of the electron possesses a structure built by subelementary particles, which are also involved in the underlying hypothetical structure of the space (the physical vacuum). The suggested electron model with a signature of anomalous magnetic moment exhibits rich oscillation and interaction behavior in this space. Two fundamental physical constants, the fine-structure constant and the Compton frequency (or wavelength), appear embedded in the electron structure and its dynamical behavior. The analysis leads to the conclusion that the Compton frequency ν_C expresses simultaneously two different features: the SPM frequency of the CL node and the first proper frequency of the oscillating electron. At the same time, the Compton wavelength λ_C expresses the length of the phase propagation of the SPM vector with a light velocity for one cycle of the SPM frequency of the CL node. This is in agreement with the relation $\lambda_C = c/\nu_C$. More details about the use of the suggested electron structure for unveiling the meaning of different physical constants are provided in the BSM hypothesis.[13] Further analysis, presented in BSM, leads to derivation of a hydrogen model possessing boundary conditions for the electronic orbits, while exhibiting the same energy levels as the Bohr atomic model. The obtained model of hydrogen further served as a base for the suggested spatial arrangement of the protons and neutrons in the atomic nuclei.[15]

Acknowledgments

I wish to express my gratitude to Mark Porringa for his useful comments and discussions related to the BSM hypothesis and particularly this monograph. Special appreciation and thanks are extended to academic Prof. Dr. Asparuh Petrakiev of the Burgas University, Bulgaria, for the organized workshop in August 2003, Varvara, Bulgaria, and to Angel Manev of the STIL at the Bulgarian Academy of Sciences for useful discussions.

Received 15 April 2002.

Résumé

Un modèle physique de l'électron est suggéré selon l'hypothèse des structures fondamentales de la matière (SFM). SFM est basé sur un concept alternatif du vide physique, en supposant que l'espace contient la structure interne en grille de nœuds, formée de particules élémentaires de super densité, qui sont également impliquées dans la structure des particules élémentaires. La structure hypothétique de grille est constituée de noeuds vibrants possédant des caractéristiques de quanta et de d'énergie. On admet que cette structure hypothétique pourrait être expliquée par la matière absente dans l'univers. La signature d'une telle matière cachée est évidente dans les courbes de rotation galactiques et dans la relation entre les masses de trous noirs super massifs au centre galactique et à la galaxie hôte. Le modèle suggéré de l'électron possède des dispositifs d'oscillation avec le moment magnétique anomal et des signatures incorporées de la longueur d'onde de Compton et de la constante de structure fine. L'analyse des interactions entre l'électron oscillant et les noeuds de la structure de grille du vide laisse prévoir l'obtention d'une signification physique pour quelques constantes fondamentales.

Endnotes

[1] Reference 13 will henceforth be referred to as BSM.

References

1. L. Ferrarese and D. Merrit, *http://arxiv.org/abs/astro-ph*, No. 0006053, v. **2,** 9 August 2000.
2. D.F. Roscoe, Phahama: J. Phys., Indian Acad. Sci. **53,** 1033 (1999).
3. T.H. Boyer, Sci. Am. (August 1985), p. 70.
4. H.E. Puthoff, Phys. Rev. A **39,** 2333 (1989).
5. *Idem*, Found. Phys. **32,** 927 (2002).
6. *Idem*, "Can the Vacuum be Engineered for Space-Flight Applications," NASA Breakthrough Propulsion Physics, Conference at Lewis Res. Centre (1977).
7. H.E. Puthoff, S. Tittle, and M. Ibison, "Engineering the Zero-Point Field and Polarizable Vacuum for Interstellar Flight," First International Workshop in Field Propulsion, University of Sussex, Brighton, U.K. (January 2001). Available: *http://www.nidsci.org/pdf/puthoff.pdf*
8. B. Haisch, A. Rueda, and H.E. Puthoff, Phys. Rev. A **49,** 678 (1994). See also Science **263,** 612 (1994).
9. F.M. Meno, Phys. Essays **4,** 94 (1991).
10. M.L. Gershteyn, L. Gershteyn, A. Gershteyn, and O. Karagioz, "Experimental Evidence that the Gravitational Constant Varies with Orientation," (2002). Available: *http://arxiv.org/abs/physics/0202058*
11. M. Ibison, H.E. Puthoff, and S.R. Little, "The Speed of Gravity Revisited," posted to LANL archives. Available: *http://lanl.arxiv.org/abs/physics/9910050*
12. S. Sarg, "New Approach for Building of Unified Theory About the Universe and Some Results." Available: *http://lanl.arxiv.org/abs/physics/0205052*
13. *Idem*, "Basic Structures of Matter," monograph (2001). Available: *http://www.helical-structures.org*; also in National Library of Canada (2002). Available: *http://www.nlc-bnc.ca/amicus/indexe.html* (AMICUS No. 27105955) (first edition)
14. *Idem*, J. Theoretics (2003), *http://www.journaloftheoretics.com/Links/Papers/Sarg.pdf*.
15. *Idem*, "Atlas of Atomic Nuclear Structures According to the Basic Structures of Matter Theory." Available: *http://www.journaloftheoretics.com/Links/papers/Sarg2.pdf*; also in National Library of Canada (2002) *http://www.nlc-bnc.ca/amicus/index-e.html* (AMICUS No. 27106037)
16. P.J. Mohr and B.N. Taylor, Rev. Mod. Phys. **72,** 351 (2000).
17. M. Wales, *Quantum Theory: Alternative Perspectives* (Shields Books). Available: *http://www.fervor.demon.co.uk*

Stoyan Sarg
CRESS/York University
206 A Petrie Bldg.
4700 Keele Street
Toronto, Ontario M3J 1P3 Canada

e-mail: stoyan@stpl.cress.yorku.ca, s.sarg@helical-structures.org